

ACCEPTED VERSION

Tess Reynolds, Alexandre Franc, ois, Nicolas Riesen, Michelle E. Turvey, Stephen J. Nicholls, Peter Hoffmann, and Tanya M. Monro

Dynamic self-referencing approach to whispering gallery mode biosensing and its application to measurement within undiluted serum

Analytical Chemistry, 2016; 88(7):4036-4040

Copyright © 2016 American Chemical Society. This document is the Accepted Manuscript version of a Published Work that appeared in final form in Analytical Chemistry copyright © American Chemical Society after peer review and technical editing by the publisher. To access the final edited and published work <http://dx.doi.org/10.1021/acs.analchem.6b00365>

PERMISSIONS

<http://pubs.acs.org/page/4authors/jpa/index.html>

The new agreement specifically addresses what authors can do with different versions of their manuscript – e.g. use in theses and collections, teaching and training, conference presentations, sharing with colleagues, and posting on websites and repositories. The terms under which these uses can occur are clearly identified to prevent misunderstandings that could jeopardize final publication of a manuscript (**Section II, Permitted Uses by Authors**).

[Easy Reference User Guide](#)

7. Posting Accepted and Published Works on Websites and Repositories: A digital file of the Accepted Work and/or the Published Work may be made publicly available on websites or repositories (e.g. the Author's personal website, preprint servers, university networks or primary employer's institutional websites, third party institutional or subject-based repositories, and conference websites that feature presentations by the Author(s) based on the Accepted and/or the Published Work) under the following conditions:

- It is mandated by the Author(s)' funding agency, primary employer, or, in the case of Author(s) employed in academia, university administration.
- If the mandated public availability of the Accepted Manuscript is sooner than 12 months after online publication of the Published Work, a waiver from the relevant institutional policy should be sought. If a waiver cannot be obtained, the Author(s) may sponsor the immediate availability of the final Published Work through participation in the ACS AuthorChoice program—for information about this program see <http://pubs.acs.org/page/policy/authorchoice/index.html>.
- If the mandated public availability of the Accepted Manuscript is not sooner than 12 months after online publication of the Published Work, the Accepted Manuscript may be posted to the mandated website or repository. The following notice should be included at the time of posting, or the posting amended as appropriate:
"This document is the Accepted Manuscript version of a Published Work that appeared in final form in [JournalTitle], copyright © American Chemical Society after peer review and technical editing by the publisher. To access the final edited and published work see [insert ACS Articles on Request author-directed link to Published Work, see <http://pubs.acs.org/page/policy/articlesonrequest/index.html>]."
- The posting must be for non-commercial purposes and not violate the ACS' "Ethical Guidelines to Publication of Chemical Research" (see <http://pubs.acs.org/ethics>).
- Regardless of any mandated public availability date of a digital file of the final Published Work, Author(s) may make this file available only via the ACS AuthorChoice Program. For more information, see <http://pubs.acs.org/page/policy/authorchoice/index.html>.

4 August, 2017

<http://hdl.handle.net/2440/100021>

A dynamic self-referencing approach to whispering gallery mode biosensing and its application to measurement within undiluted serum

Tess Reynolds^{1,*}, Alexandre François^{1,2}, Nicolas Riesen¹, Michelle E. Turvey³, Stephen J. Nicholls⁴, Peter Hoffmann^{1,3} and Tanya M. Monro^{1,2}

¹ The Institute for Photonics and Advanced Sensing (IPAS), University of Adelaide, Adelaide SA 5005, Australia

² University of South Australia, Adelaide SA 5000, Australia

³ Adelaide Proteomics Centre, University of Adelaide, Adelaide SA 5005, Australia

⁴ South Australian Health and Medical Research Institute (SAHMRI), University of Adelaide, Adelaide SA 5000, Australia

Corresponding Author

* E-mail: tess.reynolds@adelaide.edu.au; Fax: +61-8-8313-4380

ABSTRACT: Biosensing within complex biological samples requires a sensor that can compensate for fluctuations in the signal due to changing environmental conditions and non-specific binding events. To achieve this we develop a novel self-referenced biosensor consisting of two almost identically sized dye-doped polystyrene microspheres placed on adjacent holes at the tip of a micro-structured optical fiber (MOF). Here self-referenced biosensing is demonstrated with the detection of Neutravidin in undiluted, immunoglobulin-deprived human serum samples. The MOF allows remote excitation and collection of the whispering gallery mode (WGM) signals whilst also proving a robust and easy to manipulate dip-sensing platform. By taking advantage of surface functionalization techniques, one microsphere acts as a dynamic reference, compensating for non-specific binding events and changes in the environment (such as refractive index and temperature), while the other microsphere is functionalized to detect a specific interaction. The almost identical size allows the two spheres to have virtually identical refractive index sensitivity and surface area, whilst still having discernable WGM spectra. This ensures their responses to non-specific binding and environmental changes are almost identical, whereby any specific changes, such as binding events, can be monitored via the relative movement between the two sets of WGM peaks.

The phenomenon of whispering gallery modes (WGMs) within microresonators as a label free sensing modality has emerged as a powerful contender for biosensing and medical diagnostic applications^{1,2}. It has enabled unprecedented detection limits down to single molecules³, as well as the development of new *in-vivo* sensing opportunities^{1,4,5}. The spectral positions of the WGMs are determined by both the properties of the resonator (e.g. diameter, shape, refractive index) as well as the surrounding medium. The latter feature allows changes in the environment to be monitored via shifts in the spectral positions of the resonances. Surface functionalization techniques can also be utilized allowing specific interactions with desired target analytes such as proteins^{6,7}, bacteria⁸ and DNA^{9,10} to be monitored within pure samples in controlled laboratory conditions.

However, the ability of a sensor, and in particular a label free biosensor, to distinguish or eliminate unwanted fluctuations in the signal due to variations in for example temperature, surrounding refractive index or non-specific binding (NSB) is critical in real clinical samples. While it is usually possible to control the environmental conditions, such as temperature, reducing the effect of unwanted binding events in clinical samples is far more challenging. Different methods to

overcome this critical issue have been proposed, all based on surface chemistry approaches, using for example NHS esters¹¹ CM dextran¹² or polyethylene glycol (PEG).^{13,14} Integrating PEGs with silica microsphere resonators has for example allowed thrombin (~8 μ M) to be detected in tenfold diluted human serum inside a flow cell⁷. However this method requires serum to be diluted, which adds an additional processing step and reduces the concentration of the analyte by the same factor, increasing the demands on the performance of the sensor. For some applications such as the early diagnosis of myocardial infarctions in cardiology for example, where the analyte concentration is already very small¹⁵⁻¹⁷, this technique might not be suitable and alternative approaches have to be found. One such approach is to design a self-referencing sensor that allows both environmental changes and NSB events to be compensated, as is presented here.

A relatively straightforward approach of developing a self-referencing sensor is to introduce a second resonator that acts to provide a dynamic reference, similar to multiplexed sensing techniques¹⁸. Multiplexing of WGM sensors has previously been proposed conceptually¹⁸ and demonstrated in a range of geometries and configurations including passive microspheres,⁹ microdisks¹⁹ and liquid core ring resonators²⁰ and

fluorescent microspheres^{21,22}. Fluorescent or active resonators are particularly interesting in this context as they allow remote excitation of the resonator, thereby alleviating some of the practical limitations of passive resonator configurations^{9, 23-25}. Active resonators do display lower Q-factors²⁶ in comparison with passive resonators^{27,28}, however, techniques exist that can facilitate in improving the Q-factor such as operating the resonator within the stimulated emission regime²⁹ or breaking the symmetry of the resonator by placing it onto the tip of a microstructured optical fiber (MOF)³⁰. This second technique has the additional advantage of creating a robust and easy to use dip-sensing architecture¹.

In this study we demonstrate a self-referenced WGM bio-sensing platform for the specific detection and quantification of biomolecules in undiluted human serum. Our self-referenced sensing platform is based on our previously reported MOF based dip sensing active WGM platform using a 4-hole silica MOF which provides the remote excitation and collection of the WGM signal from a dye-doped polystyrene microsphere placed in one of the holes at the tip of the fiber¹. A second, almost identical microsphere (reference resonator) but differing in its surface chemistry from the sensing microsphere, is placed in an adjacent hole acting as a dynamic reference, Fig. 1 (A). The reference resonator compensates for non-specific binding as well as environmental changes, acting as a dynamic reference, while the first sphere (sensing resonator) is functionalized for detecting a specific analyte. Due to the highly sensitive nature of the resonance wavelength positions to the resonator's effective radius, differences of only nanometers allows the spectrum of each individual sphere to be clearly distinguished. The nearly-identical size of the resonators also guarantees that the two spheres have virtually identical refractive index sensitivity and surface areas, so their response to any environmental changes or NSB is almost identical, while the proximity of the spheres on the MOF's tip allows them to simultaneously experience the same local environment. Furthermore, utilizing a single gain medium for both spheres ensures that the sensing performance (sensitivity and resolution) of both resonators remain comparable, allowing the use of the relative displacement between the two sets of peaks for tracking specific binding events.

To evaluate the performance of our self-referenced fiber tip sensing platform we used a well-known specific interaction model based on biotin-Neutravidin. The Neutravidin detection limit in buffer solution (PBS) was first characterized and then repeated in Neutravidin spiked undiluted, immunoglobulin-depleted human serum samples. Following from our previous work¹, the measurements were performed in static conditions, by simply dipping the MOF tip with attached microsphere resonators into the different liquid samples as shown in Fig. 1 (B). In both sets of measurements, the non-specific binding signal was monitored using the reference resonator, while the total contribution of specific and non-specific interactions was measured by the sensing resonator. The relative movement between the two sets of resonances was then monitored.

Experimental setup, materials and method. The polystyrene microspheres (nominal diameter of $15.00 \pm 1.43 \mu\text{m}$ from Polyscience Inc) were doped with the fluorescent dye Nile Red ($\lambda_{\text{ex}} = 532 \text{ nm}$, $\lambda_{\text{em}} = 590 \text{ nm}$)³¹ using a liquid two-phase system³². Following this process, the microspheres were annealed and rinsed thoroughly to remove any trace of the organic solvent (xylene) used during the doping process, eliminating any

drift of the resonance positions over time. The surface functionalization begins with the deposition of a series of positively and negatively charged polyelectrolyte layers, poly allylamine hydrochloride (PAH) and polystyrene sulfonate (PSS) respectively³³ to form 3 layers (PAH/PSS/PAH)¹. The microspheres were then separated into two batches, sensing resonators and reference resonators, with only the sensing resonator batch being biotinylated for monitoring the specific interaction with Neutravidin. For the sensing resonators, the primary amine of the PAH layer was used to covalently immobilize biotin-D using a solution of 1-ethyl-3-(3-dimethylamionpropyl) carbodimide (EDC) and N-hydroxysuccinimide (NHS) as coupling reagents. As a final process, both the reference and sensing resonators were incubated in 2.5% casein solution for 24 hours to cover non-specific binding sites.

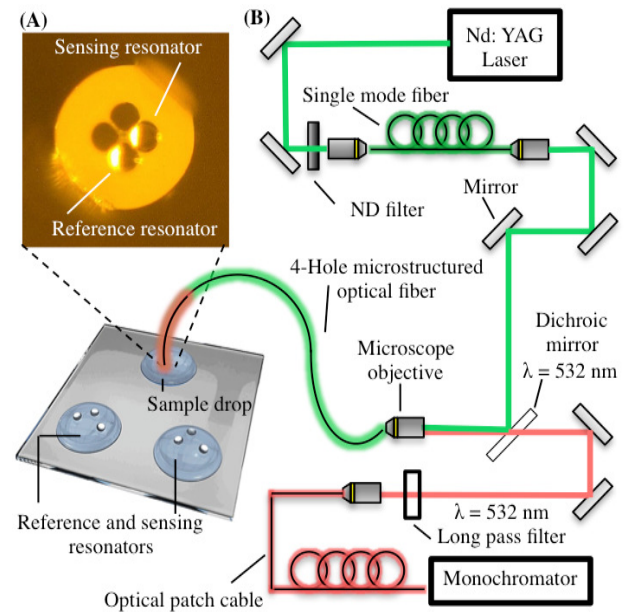


Figure 1. (A) Bright-field microscope image of two $15 \mu\text{m}$ diameter dye doped polystyrene microspheres positioned onto the tip of a 4-hole microstructured optical fiber (MOF). (B) Schematic of the optical setup.

A schematic of the optical setup is shown in Fig. 1 (B), where a frequency doubled YAG laser ($\lambda = 532 \text{ nm}$, $\sim 800 \text{ ps}$ pulse duration, 10 kHz repetition rate) was used for the excitation of the active microspheres beyond their lasing thresholds, enabling higher Q-factors as previously shown³². The light from the YAG was spatially filtered using a tapered single mode fiber (SMF28 $\text{O}_{\text{core}} = 4 \mu\text{m}$) before being coupled into the 4-hole silica MOF ($\text{O}_{\text{core}} = 7 \mu\text{m}$, $\text{O}_{\text{hole}} \sim 15 \mu\text{m}$), Fig. 1 (A). The WGM emission from the microspheres is then recaptured by the MOF and directed back through a dichroic mirror into a monochromator equipped with a cooled CCD (2048 pixels) where the WGM spectrum is recorded.

To attach the microspheres to the tip of the MOF a liquid drop containing the microspheres is placed on top of a glass coverslip and positioned on an inverted microscope. A 3 axis translational stage is used to hold and align the tip of the MOF as it is carefully lowered down into the drop of microspheres. After recording the emission spectra of free floating microspheres from both sensing and reference resonator batches, using free-space excitation and collection, one microsphere is selected from each and brought into contact with the fiber tip.

Due to the hydrophobic nature of both the MOF tip and the microspheres, the microspheres can easily be positioned in individual holes of the MOF as seen in Fig. 1 (A). It is important to note that once attached to the MOF tip, the microspheres stay in place and can be easily manipulated and dipped into other liquid droplets.

Data Analysis. All the binding kinetics presented here are presented in terms of the change in surface density of adsorbed molecules onto the surface of the resonator ($d - \text{ng}/\text{cm}^2$). This value can be estimated from the wavelength shift $\Delta\lambda$, through the effective radius increase ΔR using the following equations³⁴, where λ is the initial resonance wavelength, R is the initial resonator radius, which can be calculated from spacing of successive modes with the same polarization using Equations (2) and (3), e is the thickness of the deposited layer and n_l and n_s are the refractive indices of the layer and sphere respectively. By fitting a Gaussian function to the resonance peaks, the spectral position of the initial resonance wavelength λ_s , and subsequent positions of the peak over time can be determined.

$$\frac{\Delta\lambda}{\lambda} = \frac{\Delta R}{R} = \frac{n_l e}{n_s R} \quad (1)$$

$$R = \frac{\lambda_{m+1} m}{2\pi n_s} \quad (2)$$

$$m = \frac{\lambda_{m+1}}{\lambda_m - \lambda_{m+1}} + 1 \quad (3)$$

Where m is the mode number and λ_{m+1} and λ_m are the wavelengths of two successive modes with the same polarization.

$$d = \frac{M}{N_A \sigma_p} \quad (4)$$

$$\sigma_p^{-1} = \frac{n_s}{n_m} \frac{\alpha_{ex}}{\epsilon_0 (n_s^2 - n_m^2)} \frac{1}{\Delta R} \quad (5)$$

$$\alpha_{ex} = \frac{\epsilon_r - 1}{\epsilon_r + 2} \frac{3M\epsilon_0}{N_A \rho_m} \quad (6)$$

Here, M is the molecular weight, N_A is Avogadro's number, σ_p is the projected area of the adsorbed molecule, α_{ex} is the excess polarizability, which to a first approximation can be calculated using the Clausius-Mossotti formula (Eq. 6), ϵ_0 is the free-space permittivity, ϵ_r is the dielectric function of the molecule considered, ρ is the mass density ($\rho = 1.37 \text{ g}/\text{cm}^3$ for most proteins³⁵) and n_m and n_s are the refractive indices of the surrounding environment and microsphere, respectively. Calculating the surface density allows comparison with other techniques and sensing geometries as it removes the dependence on the geometry as well as the refractive index sensitivity of the sensor being considered.

Results and discussion. Figure 2 (A) and (B) show the typical WGM spectra of the two-microsphere system above and below the lasing threshold respectively. Below the lasing threshold the individual resonances of each sphere cannot be distinguished. However, operating the spheres above their lasing threshold not only allows the spectra of the individual spheres to be clearly identified, but also improves resolution, enabling lower detection limits to be reached¹. The resonance spectra

typically do not overlap, when operated in the stimulated emission regime as even a minute deviation in diameter between the two microspheres results in a discrepancy between the resonances. In this configuration, the spheres can either be tracked individually by following an individual peak or alternatively, by performing a convolution on the two resonator comb-like WGM spectra as both spheres respond to the same environment, Fig. 2 (C).

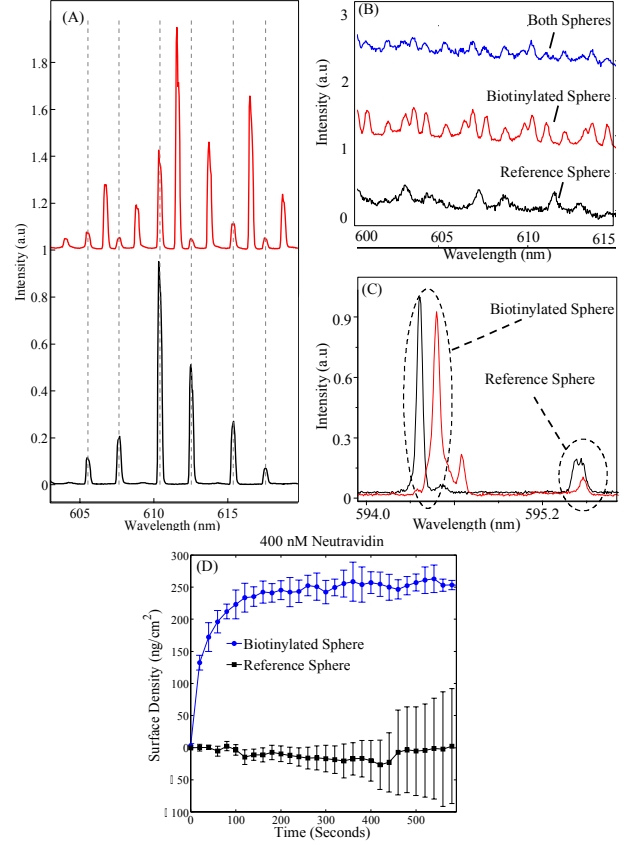


Figure 2. (A) Whispering gallery mode spectrum of the reference sphere alone (black trace) and both the biotinylated and reference spheres (red trace) attached to the tip of the microstructured optical fiber (MOF), operating above the lasing threshold. Both spheres are $15 \mu\text{m}$ in diameter. (B) Whispering gallery mode spectrum of the reference (black), biotinylated (red) and both the reference and biotin spheres attached to the tip of the microstructured optical fiber below the lasing threshold. (C) Comparison of the whispering gallery mode spectra of both the reference and biotinylated microspheres attached to the tip of the MOF when initially in water (black trace) and after dipping into Neutravidin solution for 8 minutes (red trace). (D) Binding kinetic of Neutravidin onto the biotinylated sphere (blue trace) and reference sphere (black trace).

Once both spheres are attached, spectra are taken at 20 second intervals as the fiber is moved into the Neutravidin solution. Fig. 2 (D) shows the response of both microspheres when placed in 400 nM Neutravidin solution. From the responses of the two spheres it is clear that binding is occurring on the biotinylated sphere, with equilibrium being reached after approximately 200 seconds, while the reference sphere spectrum remains relatively stable throughout the measurement with deviations towards the end of the measurement. This result is consistent with our previous demonstrations of fiber tip¹ and

fluorescent microcapillary³⁶ sensing. We also note that the presence of the reference sphere does not have any effect on the biotinylated sphere's performance. As such, the process is repeated for decreasing Neutravidin concentrations, with each concentration being measured 3 times. Each individual measurement is completed with a new set of spheres. No deviation is observed for the reference spheres during the Neutravidin measurements, and for simplicity only the binding kinetic of the biotinylated sphere is shown for each of the concentrations in Fig. 3, where the error bars have been calculated from the standard deviation of all three trials completed for each concentration.

After completing these initial trials in PBS, the same experimental procedure was used to investigate the sensor's response in human serum samples. Drops of each of the sphere populations were once again placed on top of a glass cover slip, with a single sphere from each subsequently attached to the fiber tip, along with 30 μ L drops of 1:20 (v/v) and 1:40 (v/v) diluted human serum without Neutravidin added. The response of the individual spheres in the sensor is displayed in Fig. 4. Examining Fig. 4, it is clear that significant adsorption is occurring in both sphere populations, however there is a reduction in the adsorption of the biotinylated sphere as the dilution of the sample increases, Fig. 4(A), while the reference sphere's response remains almost unchanged, Fig 4(B). Without any added Neutravidin in the diluted serum sample, these results indicate that there is another molecule present in the serum that is interacting and binding to the biotinylated sphere surface. It has been reported that immunoglobulin can interact with biotin, resulting in false positive results for similar biotinylated-based immunoassays³⁷.

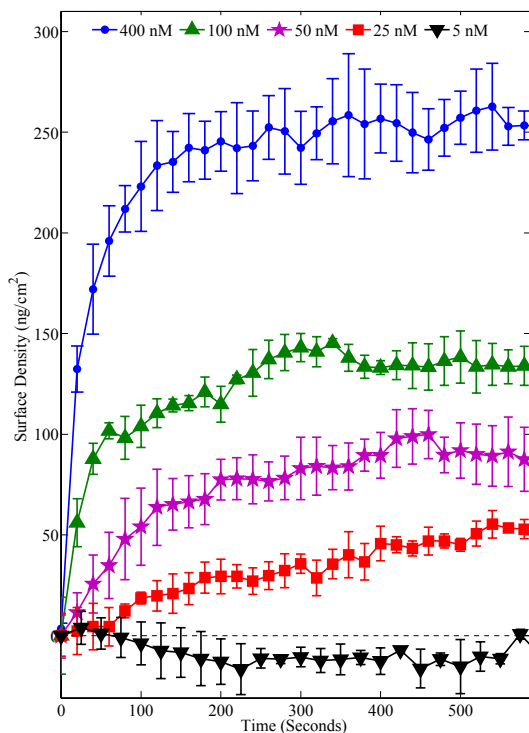


Figure 3. Binding kinetic of Neutravidin on a 15 μ m biotinylated microsphere of five different concentrations 5-400 nM.

Therefore, to avoid such false positive results while using biotin-Neutravidin as a specific interaction model, the immuno-

globulin was removed from our serum samples by brief incubation and pull-down with Protein A/G-conjugated sepharose beads. Four pull-downs with Protein A/G beads were required to ensure that the false positive signal on the biotinylated microspheres was reduced to zero using undiluted serum while significant adsorption on the reference microspheres due to the non-specific binding of the large protein content of the serum was still present.

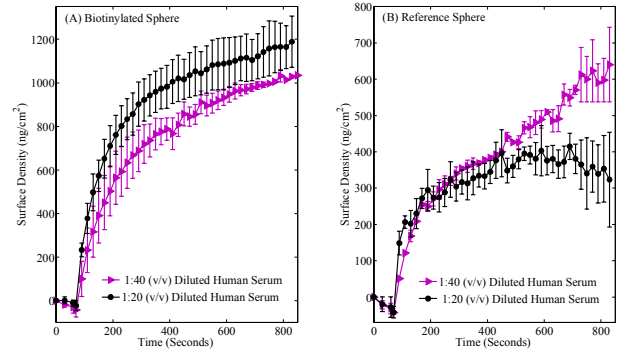


Figure 4. Binding kinetic of a sensing resonator (A) and reference resonator (B) attached to the tip of a fiber dipped into two human serum samples of different dilution.

Tests were repeated with pure human serum, with the Immunoglobulin removed, avoiding the unwanted binding between the Immunoglobulin and the sensing resonator, but spiked with a known Neutravidin concentration. The results for the lowest concentration tested are shown in Fig. 5.

For all the tests performed, the reference resonator exhibited a similar behavior characterized by a sharp wavelength shift, or increase of the surface density, due to the large NSB component introduced by the serum, despite the use of casein as a blocking reagent. This highlights the fact that blocking solutions such as caseine, Bovine Serum Albumin and alike are inherently inefficient in preventing NSB in complex biological samples. The biotinylated microspheres however showed a steady increase in the surface density beyond the initial WGM wavelength shift due to the high refractive index of the serum, which characterizes the Langmuir adsorption of the Neutravidin onto the biotinylated resonator surface, down to 25 nM Neutravidin concentration. Once the contribution from the NSB is subtracted from the biotinylated microsphere response a perfect correlation between the Neutravidin binding kinetic in PBS and undiluted serum was reached as shown in the Fig. 5 (D) and 5 (E). For the lowest concentration tested (5 nM), no unambiguous positive detection of Neutravidin can be observed whether in PBS or undiluted serum.

In conclusion, this simple approach of using two almost identical microspheres, differing by their surface functionalization, for self-referencing purposes has shown that specific detection and quantification in undiluted serum sample can be realized. The reference microsphere allows for the compensation of the non-specific binding, enabling the quantification of the binding of the analyte onto the sensing resonator surface in complex biological samples to be correlated with what happens with the same target analyte in buffer solution.

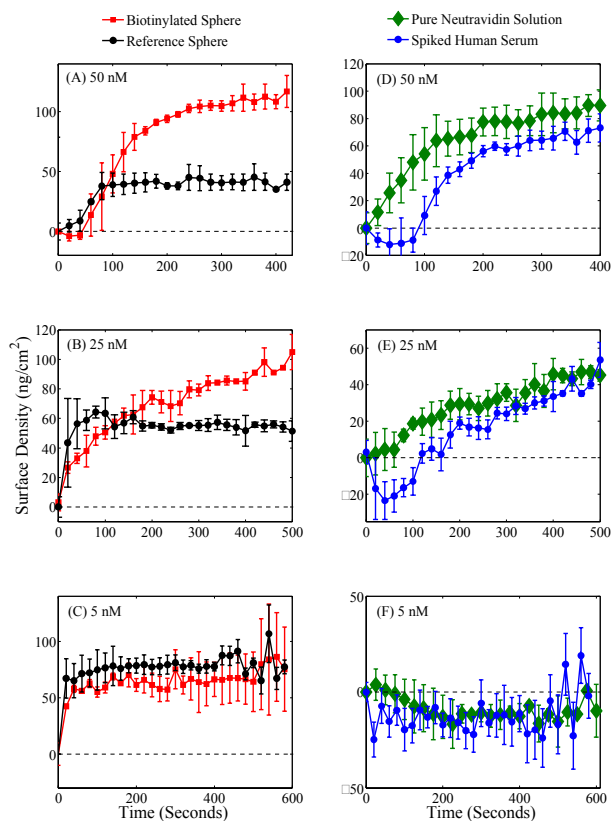


Figure 5. Individual sphere responses of the biotinylated (red trace) and reference (black trace) spheres when dipped into human serum samples spiked with (A) 50 nM, (B) 25 nM and (C) 5 nM concentrations of Neutravidin. (D)-(F) Comparison of the corrected binding kinetic of the sensor in the spiked human serum samples (blue trace) with binding kinetic in the pure Neutravidin solution (green trace).

While for the sake of the specific interaction model used for this demonstration, the immunoglobulin had to be removed, one can appreciate that this approach can still be used for the detection of other more relevant biomolecules in serum, without having to process the serum by removing the immunoglobulin once antibodies are used to target a specific biomolecule instead of biotin. Furthermore, one can also expand this concept to multiplexed detection of different biomolecules simultaneously, taking advantage of the multiple holes on the MOF to accommodate microspheres targeting different biomolecules.

AUTHOR INFORMATION

Corresponding Author

* E-mail: tess.reynolds@adelaide.edu.au

ACKNOWLEDGMENT

The authors acknowledge the support of T. M. Monro's ARC Georgina Sweet Laureate Fellowship. This work was performed in part at the Optofab node of the Australian National Fabrication Facility utilizing Commonwealth and SA State Government funding. Authors thank Roman Kostecki, Erik Schartner, Peter Henry and Alastair Dowler for help with the silica microstructured fiber fabrication.

REFERENCES

- (1) François, A.; Reynolds, T.; Monro, T. M. *Sensors* **2015**, *15*, 1168-1181.
- (2) Agarwal, M.; Teraola, I.; *Anal. Chem.* **2015**, *87*, 10600-10604.
- (3) Baaske, M. D.; Foreman, M. R.; Vollmer, F. *Nat. Nanotechnol.* **2014**, *9*, 933-939.
- (4) Humar, M.; Yun, S. H.; *Nature Photonics* **2015**, *9*, 572-576.
- (5) Schubert, M.; Steude, A.; Liehm, P.; Kronenberg, N. M.; Karl, M.; Campbell, E. C.; Powis, S. J.; Gather, M. C. *Nano. Lett.* **2015**, *15*, 5647-5652.
- (6) Ballard, Z.; Baaske, M. D.; Vollmer, F.; *Sensors* **2015**, *15*, 8968-8990.
- (7) Pasquardini, L.; Berneschi, S.; Barucci, A.; Cosi, F.; Dalla-piccola, R.; Insinna, M.; Lunelli, L.; Conti, G. N.; Pederzoli, C.; Salvadori, S.; Soria, S. *J. Biophotonics* **2013**, *6*, 178-187.
- (8) Anderson, M. E.; O'Brien, E. C.; Grayek, E. N.; Hermansen, J. K.; Hunt, H. K. *Biosensors* **2015**, *5*, 562-576.
- (9) Vollmer, F.; Arnold, S.; Braun, D.; Teraoka, I.; Libchaber, A. *Biophys. J.* **2003**, *85*, 1974-1979.
- (10) Fan, X. D.; Sutter, J. D.; White, I. M.; Zhu, H. Y.; Shi, H. D.; Caldwell, C. W. *Biosens. Bioelectron.* **2008**, *23*, 1003-1009.
- (11) Masson, J. F.; Battaglia, T. M.; Cramer, J.; Beaudoin, S.; Sierks, M.; Booksh, K. S. *Anal. Bioanal. Chem.* **2006**, *386*, 1951-1959.
- (12) Bolduc, O. R.; Pelletier, J. N.; Masson, J. F. *Anal. Chem.* **2010**, *82*, 3699-3706.
- (13) Ostuni, E.; Chapman, R. G.; Holmin, R. E.; Takayama, E.; Whitesides, G. M. *Langmuir* **2001**, *17*, 5605-5620.
- (14) Wang, F.; Anderson, M.; Bernards, M. T.; Hunt, H. K. *Sensors* **2015**, *15*, 18040-18060.
- (15) Konstantinides, S.; Geibel, A.; Olschewski, M.; Kasper, W.; Hruska, N.; Jäckle, S.; Binder, L.; *Circulation.* **2002**, *106*, 1263-1268.
- (16) Maisel, A.; *Circulation.* **2002**, *105*, 2328-2331.
- (17) Ridker, P. M.; *Circulation.* **2001**, *103*, 1813-1818.
- (18) Boriskina, S. V.; Dal Negro, L. *Opt. Lett.* **2010**, *35*, 2496-2498.
- (19) Qavi, A. J.; Kindt, J. T.; Gleeson, M. A.; Bailey, R. C. *Anal. Chem.* **2011**, *83*, 5949-5956.
- (20) White, I. M.; Oveys, H.; Fan, X.; Smith, T. L.; Zhang, J. *Appl. Phys. Lett.* **2006**, *89*, 191106.
- (21) Huckabay, H. A.; Wildgen, S. M.; Dunn, R. C. *Biosens. Bioelectron.* **2013**, *45*, 223-229.
- (22) Kim, D. C.; Armendariz, K. P.; Dunn, R. C. *Analyst.* **2013**, *138*, 389-3195.
- (23) Ksendov, A.; Lin, Y. *Opt. Lett.* **2005**, *30*, 3344-3346.
- (24) Gorodetsky, M. L.; Ilchenko, V. S. *J. Opt. Soc. Am. B.* **1999**, *16*, 147-154.
- (25) Guo, Z.; Quan, H.; Pau, S. *J. Phys. D: Appl. Phys.* **2006**, *39*, 5133-5136.
- (26) Riesen, N.; Reynolds, T.; François, A.; Henderson, M. R.; Monro, T. M. *Opt. Express.* **2015**, *23*, 28896-28904.
- (27) Vernooy, D. W.; Ilchenko, V. S.; Mabuchi, H.; Steed, E. W.; Kimble, H. J. *Opt. Lett.* **1998**, *23*, 247-249.
- (28) Gorodetsky, M. L.; Savchenkov, A. A.; Ilchenko, V. S.; *Opt. Lett.* **1996**, *21*, 453-455.
- (29) Klimov, V. I.; Mikhailovsky, A. A.; Xu, S.; Malko, A.; Hollingsworth, J. A.; Leateherdale, C. A.; Eicher, H. J.; Bawendi, M. G. *Science* **2000**, *290*, 314-317.
- (30) François, A.; Rowland, K. J.; Afshar, S. V.; Henderson, M. R.; Monro, T. M. *Opt. Express.* **2013**, *21*, 22566-22577.
- (31) Greenspan, P.; Mayer, E. P.; Fowler, S. D. *J. Cell. Bio.* **1985**, *100*, 965-973.
- (32) François, A.; Riesen, N.; Ji, H.; Afshar, V. S.; Monro, T. M. *Appl. Phys. Lett.* **2015**, *106*, 031104.
- (33) Decher, G. *Science* **1997**, *275*, 1232-1237.

- (34) Arnold, S.; Khoshsima, M.; Teraoka, I.; Holler, S.; Vollmer, F. *Opt. Lett.* **2003**, *28*, 272-274.
- (35) Schweiger, G.; Horn, M. *J. Opt. Soc. Am. B.* **2006**, *23*, 212-217.
- (36) Lane, S.; West, P.; François, A.; Meldrum, A. *Opt. Express.* **2015**, *23*, 2577-2590.
- (37) Chen, T.; Hedman, L.; Mattila, P.S.; Jartti, L.; Jartti, T.; Ruuskanen, O.; Soderlund-Venermo, M.; Hedman, K. *PLoS One* **2014**, *7*, 43276.